RETRACTION
https://doi.org/10.1071/CH18568_RE

Retraction notice to 'Crystal structures and anti-colon cancer activity of two lanthanide complexes with O-donor diacetone ligands'

Gang Chen, Chang-Hong Yu, Xin Lv, Bing Qiu and Wei Jiang

Australian Journal of Chemistry (2019)
doi:10.1071/CH18568

Refers to: RETRACTED: Crystal Structures and Anti-Colon Cancer Activity of Two Lanthanide Complexes with O-Donor Diacetone Ligands, published 15 March 2019, doi.org/10.1071/CH18568. Gang Chen, Chang-Hong Yu, Xin Lv, Bing Qiu and Wei Jiang.

After due consideration of issues raised with respect to this paper, the Editors-in-Chief and the authors agree to retract the paper from *Australian Journal of Chemistry*. Reason: Upon review of the submission history for the manuscript, the *Australian Journal of Chemistry* Editors and Publisher found indications that the peer review process is likely to have been compromised by the submission of reviews through suspected fabricated reviewer accounts.

The Editors-in-Chief and Journal Publisher have determined these are grounds for retraction, according to the international guidelines established by the Committee on Publication Ethics. We regret the academic record was compromised and apologise for any inconvenience this may have caused.

Chen G *et al.* (2023) *Australian Journal of Chemistry*
76(4), 231. doi:10.1071/CH18568_RE

CSIRO PUBLISHING

Aust. J. Chem.
https://doi.org/10.1071/CH18568

Full Paper

Crystal Structures and Anti-Colon Cancer Activity of Two Lanthanide Complexes with O-Donor Diacetone Ligands

Gang Chen,[A,D] *Chang-Hong Yu*,[A,D] *Xin Lv*,[B] *Bing Qiu*,[C] *and Wei Jiang*[A,E]

[A]Department of Gastroenterology, First Affiliated Hospital of Jiamusi University, Jamusi, Heilongjiang 154002, China.
[B]Department of General Surgery, First Affiliated Hospital of Jiamusi University, Jamusi, Heilongjiang 154002, China.
[C]Department of Gastroenterology, Heilongjiang Provincial Hospital, Harbin, Heilongjiang 150036, China.
[D]These authors contributed equally to this work.
[E]Corresponding author. Email: wei_jiang666@126.com

Two new lanthanide–organic complexes, $[Ho_4(\mu_3\text{-}OH)_4\{(\mu\text{-}O)\text{-}\eta^2\text{-}acac\}_4(\eta^2\text{-}acac)_4]\cdot(C_7H_8)_{0.5}$ (**1**, acac = acetylacetone) and $[Nd_2(phen)\{(\mu\text{-}O)\text{-}\eta^2\text{-}phacac\}_4(SO_4)]$ (**2**, phen = phenanthroline, phacac = phenylazoacetylacetone) with different structural architectures have been obtained via a ligand-directed synthesis method. The molecular networks of the as-prepared compounds were determined by single crystal X-ray diffraction analysis and their phase purities have been confirmed via power X-day diffraction analysis. Furthermore, the crystal size for the as-prepared two complexes could be conveniently decreased to nanometre size via a grinding method. The anticancer activities of the as-prepared two nanostructures have been evaluated via the 3-(4,5-dimethylthiazol-2-yl)-2,5-diphenyltetrazolium bromide (MTT) assay against the human colon cancer cell line SW60.

Manuscript received: 16 November 2018.
Manuscript accepted: 13 February 2019.
Published online: 15 March 2019.

Introduction

As one of the most life-threatening diseases, cancer leads to millions of deaths every year. Since the last century, a large number of natural and chemical drugs have been discovered and developed with the aim of curing cancer with better therapeutic efficiency and fewer side effects.[1] Although the discovery of the chemotherapeutic agent cisplatin was more than 30 years ago, it is still one of the most effective and world's best-selling anticancer drugs. However, cisplatin suffers from some drawbacks such as drug resistance, general toxicity, and serious side effects, which limits its large dose of administration.[2] The encountered clinical problems of recent chemotherapeutic drugs have given rise to the development of novel anticancer agents based not only on the use of noble metals, but also on the use of essential metallic elements. Recent literature has revealed that many metal coordination complexes are potent growth inhibitors of human cancer cells and have been extensively investigated and evaluated in vitro and in vivo.[3–5]

On the other hand, the construction of coordination polymers that are composed of metal ions/nodes and organic ligand connectors via the self-assembly approach has gained great interest in the last few decades because these materials could inherit the properties from both the inorganic and organic motifs, which see them potentially applied in many important domains ranging from guest adsorption to drug delivery.[6–12] Recent studies have revealed that some lanthanide coordination compounds could be used as anticancer reagents. For instance, Li and co-workers have prepared a La^{III}-based coordination polymer using a bifunctional organic ligand, which could be used for the human Caucasian lung carcinomaablation of A549 cells.[10] Kumaresan et al. studied the anticancer activities of a series of lanthanide complexes based on a Schiff base ligand, which found that the Eu^{III} and Nd^{III} complexes were more active than the corresponding Gd^{III}, Sm^{III}, and Tb^{III} complexes and the free ligand on both the cancer cell lines.[13] However, due to their micro-region crystal size, coordination polymers usually show very low solubility in common organic solvents which limit their potential applications in several desirable biological applications such as drug delivery and treatment of cancer.[14] In this study, two new lanthanide–organic complexes, $[Ho_4(\mu_3\text{-}OH)_4\{(\mu\text{-}O)\text{-}\eta^2\text{-}acac\}_4(\eta^2\text{-}acac)_4]\cdot(C_7H_8)_{0.5}$ (**1**, acac = acetylacetone) and $[Nd_2(phen)\{(\mu\text{-}O)\text{-}\eta^2\text{-}phacac\}_4(SO_4)]$ (**2**, phen = phenanthroline, phacac = phenylazoacetylacetone) with different structural architectures have been obtained via a ligand-directed synthesis method. The molecular structures of the as-prepared complexes were determined by single crystal X-ray diffraction (SCXRD) studies and their phase purities have been confirmed by power X-day diffraction analysis (PXRD). In complex **1**, four lanthanide atoms, four μ_3-O atoms, and eight acac ligands make up the peripheral part of the cubane-like $Ho_4(\mu_3\text{-}OH)_4^{8+}$ cluster core with the acac ligands showing two different types of structural conformations. In complex **2**, the

Table 1. Crystal data and structure refinements for 1 and 2

Parameter	1	2
Empirical formula	$C_{50.5}H_{70}Ho_4O_{20}(C_7H_8)_{0.5}$	$C_{54}H_{38}N_4NdO_6S$
Formula weight	1702.85	1015.18
Temperature [K]	293(2)	289.3
Crystal system	tetragonal	monoclinic
Space group	$I4_1/a$	$P2_1/n$
a [Å]	14.0132(3)	13.4241(8)
b [Å]	14.0132(3)	14.2142(10)
c [Å]	32.416(5)	24.9296(14)
α [deg.]	90	90
β [deg.]	90	93.131(5)
γ [deg.]	90	90
Volume [Å^3]	6365.5(10)	4749.8(5)
Z	4	4
ρ_{calc} [g cm^{-3}]	1.777	1.[illegible]
μ [mm^{-1}]	4.984	1.1[illegible]
2θ range for data collection [deg.]	6.334 to 53.024	[illegible]78 to 49.[illegible]8
Reflections collected	19995	[illegible]7282
Independent reflections	3244 (R_{int} 0.0693)	8335 ([illegible].0469)
Data/restraints/parameters	3244/20/186	8335/[illegible]/613
Goodness-of-fit on F^2	1.178	[illegible].083
Final R indexes [$I \geq 2\sigma(I)$]	R_1 0.0248, ωR_2 0.0525	0.[illegible]736, ωR_2 0.2209
Final R indexes [all data]	R_1 0.0313, ωR_2 0.0536	[illegible].0958, ωR_2 0.2458
Largest diff. peak/hole [e Å^{-3}]	0.51/−0.39	1.91/−0.80
CCDC	1878788	1878789

central Nd^{3+} ion is eight-coordinated by four O atoms from two different phacac ligands and four N atoms from two different phen ligands, giving a square antiprism coordination geometry. Furthermore, the crystal size of the as-prepared two com[illegible]xes could be conveniently decreased to nanometre dim[illegible]ions [illegible] a grinding method. The anticancer activities of the as-prepared two nanostructures have been evaluated via the [illegible]4,5-dimethylthiazol-2-yl)-2,5-diphenyltetrazolium bromide (MTT) assay against the human colon cancer cell line [illegible]60.

Experimental

Materials and Instrumentation

All solvents and chemicals were acquired commercially from the Merck and Aldrich reagent companies and used as received. A Perkin Elmer CHN elemental analyser was used to acquire the CHN content in the as-prepared two complexes. Thermogravimetric analysis (TGA) was carried out on a NetzschSTA499C integration thermal analyser in the temperature range from 30 to 800°C at a heating rate of 10°C min^{-1} under a nitrogen atmosphere. Powder X-ray diffraction (PXRD) analyses were recorded on a PANalytical X'Pert Pro powder diffractometer with Cu Kα radiation (λ 1.54056 Å) with a step size of 0.05°. The morphologies of the obtained nanoparticles were examined with a TESCAN MIRA3 field emission scanning electron microscope.

*Synthesis of Compounds **1** and **2***

To a solution of $HoCl_3{\cdot}6H_2O$ (0.1 mmol, 0.38 g) in 10 mL of cold water was slowly added a solution of NH_4acac (aq, 1 mol L^{-1}, 50 mL) with stirring. $NH_3{\cdot}H_2O$ (1 mol L^{-1}) was added to modulate the pH value to 7.5–8.0, forming white precipitates. After ~3 h of stirring, the white precipitates were filtered off, washed with water, and dried in air to give ~54 % yield (based on $HoCl_3{\cdot}6H_2O$). Recrystallisation of the white precipitates in toluene (5 mL) resulted in block colourless [illegible]s of **1**. Anal. Calc. for **1** ($C_{54}H_{76}O_{20}Ho_4$): C 38.04, H 4.49. Found: C 37.89, H 4.16 %. ν_{max} (KBr pellet)/cm^{-1} 3233(s), 1648(s), 1565(s), 1425(s), 1297(s), 1238(m), 1143(s), 1027(m), 919(m), 661(w).

Neodymium(III) sulfate octahydrate (0.072 g, 0.1 mmol) in anhydrous ethanol (10 mL) was added dropwise to a stirred solution of 1,3-diphenyl-1,3-propanedione (0.168 g, 0.75 mmol) and 1,10-phenanthroline (0.0495 g, 0.25 mmol) in anhydrous ethanol (15 mL) at 50°C. The pH value of the reaction mixture was adjusted to ~6 with aqueous ammonia. The resulting solution was stirred at 50°C for another 5 h and left sitting at room temperature overnight. It was then filtered to obtain the block-shaped crystalline products (yield 49 % based on the 1,10-phenanthroline ligand). Anal. Calc. for $C_{54}H_{38}N_4NdO_6S$: C 63.89, H 3.77, N 5.52. Found: C 63.14, H 3.82, N 5.51 %. ν_{max} (KBr pellet)/cm^{-1} 3108 (w), 3057 (w), 2922 (s), 1611 (m), 1481 (m), 1356 (s), 1328 (s), 1164 (s), 1035 (m), 910 (w)

X-Ray Crystallography

Suitable single crystals of **1** and **2** were carefully selected under an optical microscope and glued to thin glass fibres. Structural measurements were performed with a computer controlled Oxford diffractometer with graphite-monochromated Mo Kα radiation (λ 0.71073 Å) at 293(2) K using the *CrysAlisPro* software system (version 1.171.34.40). The structure was solved by direct methods using the program *SHELXS-97*. The refinement and all further calculations were carried out using *SHELXL-97* based on the full-matrix least-squares method.[15] Hydrogen atoms were calculated and refined in riding mode and the non-hydrogen atoms were treated anisotropically. Crystal data, as well as details of data collection and refinements of **1** and **2** are summarised in Table 1.

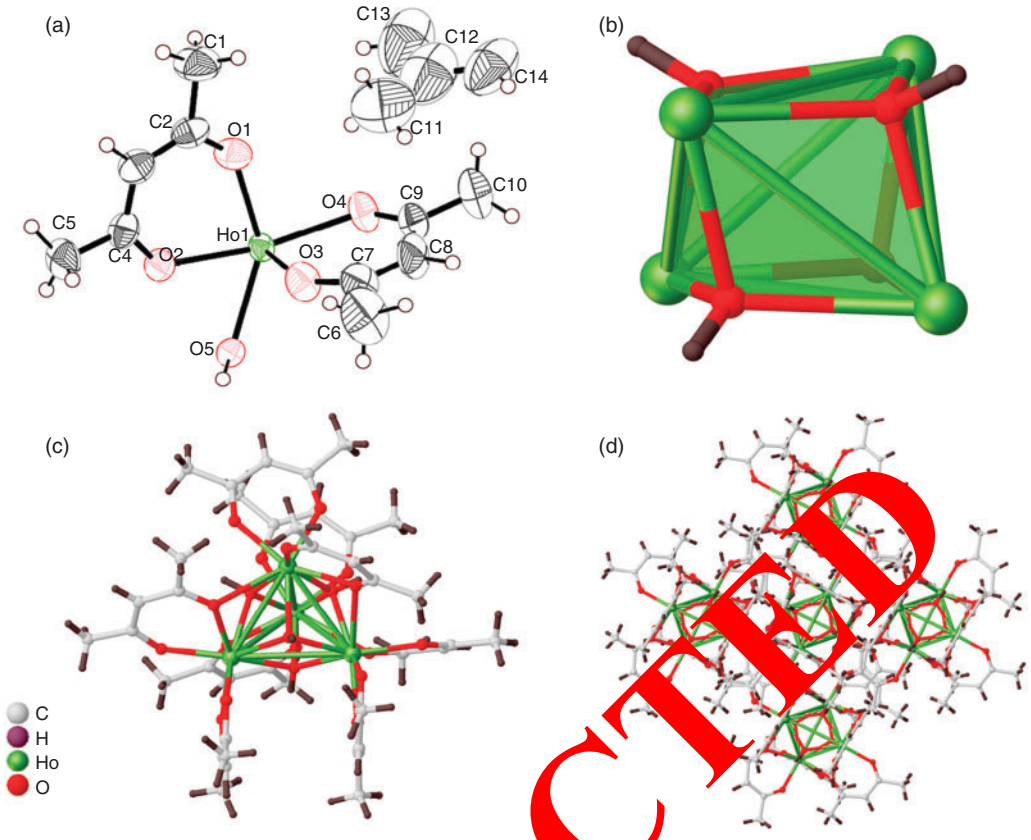

Fig. 1. (a) View of the asymmetric unit of **1**. (b) The 1D chain-like network of **1**. (c) The 3D supermolecular network of **1** via packing of the 1D chain-like network. (d) View of the π–π interactions between adjacent chains.

Antitumour Activity

The MTT assay was used to examine the viability enhancement against the two as-synthesised compounds. Typically, in 96-well plates was seeded cancer cells at a density of 5×10^3 cells well^{-1}. The cells were then exposed to various concentrations (ranging between 0–10 μg mL^{-1}) of compound **1** or **2** for 48 h after 24 h of incubation. After the incubation, the medium containing the compounds was removed followed by the addition of 10 μL of MTT (5 mg mL^{-1} phosphate buffered saline, PBS) to each well and incubated at 37°C for 3 h. DMSO (100 μL) was then added to dissolve the purple crystals. The optical density (OD) value at 570 nm was recorded using a spectrophotometer (Bio-Rad, Hercules, CA, USA). Each concentration was tested three times and five replica wells were used for controls. By taking the control wells as 100 % of viability, the absorption values of each well were expressed as the percent of cell viability. The IC_{50} values (concentration required to inhibit 50 % cell growth) were obtained from the dose–response curves.

The SW60 colon cancer cells were treated with nanocrystalline **1** and **2**, respectively, and the apoptosis levels among total cells were then measured by a FITC Annexin V Apoptosis Detection Kit I (BD Biosciences, New Jersey, USA) according to the manufacturer's protocol. In brief, the SW60 cells were planted on six well plates (5×10^5 cells well^{-1}) and incubated at 37°C with 5 % CO_2 for 12 h. After replacing the fresh medium, nanocrystalline **1** and **2** at a concentration of $1 \times IC_{50}$ was added DMSO was added as the negative control. After 24 h, the SW60 cells were collected into Eppendorf (EP) tubes. The cells were washed three times with phosphate buffered saline (PBS) and labelled with fluorochrome-conjugated Annexin V and Propidium Iodide dyes for 30 min. Finally, the percentage of apoptotic cells were analysed by flow cytometry at an excitation wavelength of 488 nm and emission wavelengths of 525 and 625 nm.

The influence of nanocrystalline **1** and **2** on reactive oxygen species (ROS) production in treated SW60 cells was detected with the Reactive Oxygen Species Assay Kit in accordance with the manufacturer's protocol. The SW60 cells were seeded on six-well plates (5×10^5 cells well^{-1}) and incubated with or without nanocrystalline **1** or **2** for 24 h. After incubation, the SW60 cells were collected and washed three times with PBS, followed by labelling with H2DCF-DA dye (20 μM). The cells were then incubated at 37°C in 5 % CO_2 for 30 min and harvested. All the samples were analysed by flow cytometry (FACS Calibur, BD Biosciences, USA) at an excitation wavelength of 488 nm and emission wavelengths of 525 and 625 nm.

Results and Discussion

*Structural Description of Compounds **1** and **2***

The title complex **1** was synthesised by reaction of NH_4acac and $HoCl_3 \cdot 6H_2O$ with $NH_3 \cdot H_2O$ as the pH modulator. Its crystal structure was determined by SCXRD at room temperature. The crystal solution and refinements study reveal that compound **1** locates in the tetragonal space group $I4_1/a$, and exists in a discrete cluster-based structure. There is one crystallographically independent Ho^{3+} ion, one bridging μ_3-OH group, two chelating acac ligands, and half a lattice toluene molecule in the molecular unit (Fig. 1a). The eight coordinated $\{HoO_8\}$ bicapped trigonal prism arrangement of the Ho^{3+} ion is completed by five O atoms from three chelating acac ligands and three O atoms from the

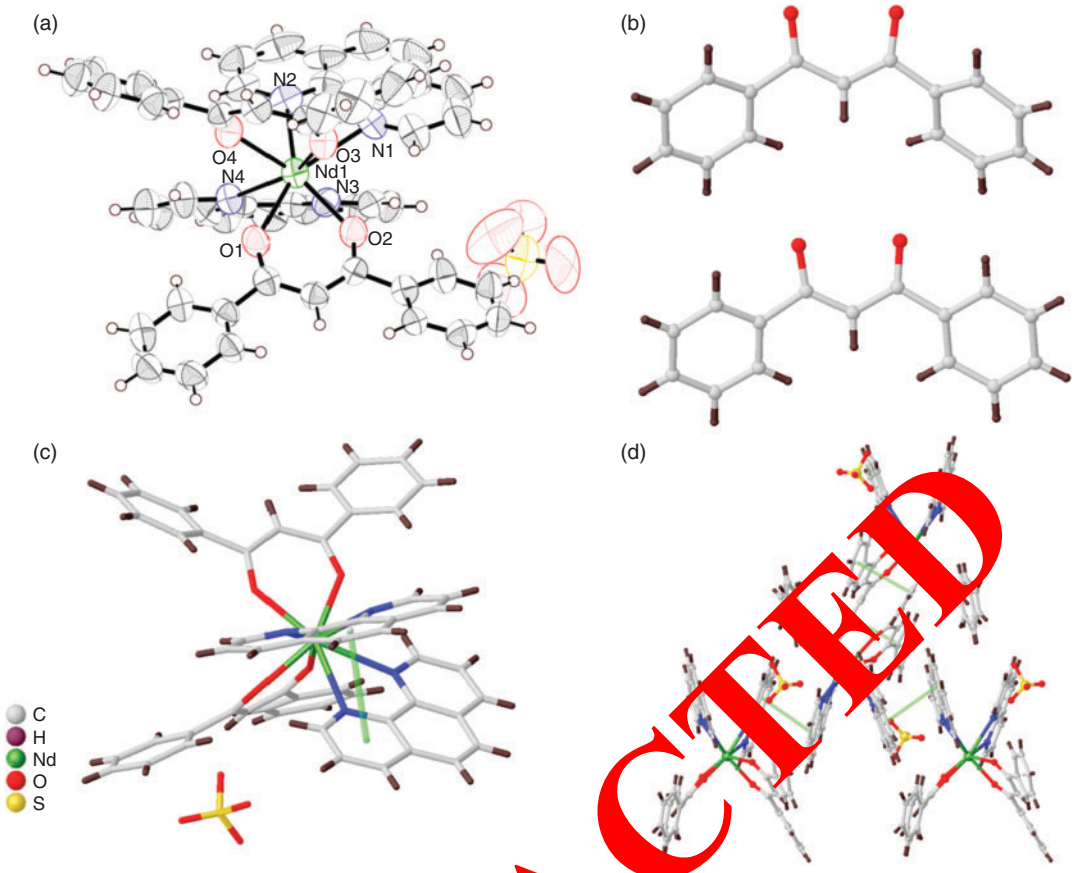

Fig. 2. (a) View of the asymmetric unit of **2**. (b) The molecular co… of the phacac ligands. (c) View of the intramolecular π–π interactions in **2**. (d) View of the intermolecular π–π interactions.

μ_3-bridging OH groups. In addition, the valence for t… O ato… in the OH group of complex **1** has been calcula…ed to be –…sing the *Bond Valence Sum* (BVS) software, w… has been con-firmed to be a reasonable method for obta…ining … valencey of deprotonated water molecules.[16] Th… Ho–O bond …ances are in the region of 2.227(3) to 2.400(3) Å, which all locate in the normal range of the Ho–O bond d… …es in other Ho^{3+}-based coordination complexes.[17] Four μ_3-bri…ing OH groups connect with four symmetry related Ho^{3+} i… to result in the $[Ho_4((\mu_3\text{-}OH)_4)]^{8+}$ clus… core, …hich four μ_3-OH groups and four Ho^{3+} ions are alterna…y arranged at the corners of the distorted Ho_4O_4 cubane-like …ster (Fig. 1b). The two acac ligands in the molecular unit demonstrate two different coordination modes: one shows a μ_1-η^1:η^1 coordination mode and the other one reveals a μ_2-η^1:η^2 pattern. The $[Ho_4((\mu_3\text{-}OH)_4)]^{8+}$ cluster is surrounded by eight acac ligands to afford the molecular structure of **1**, which is further stacked into the 3D supermolecular network via van der Waals interactions (Fig. 1c, d). The structure of **1** is similar to the reported Er^{3+}-based coordination complex with different amounts of lattice solvent.[18]

The SCXRD study reveals that compound **2** belongs to the monoclinic crystal system, space group *P*21/*n* and demonstrates a discrete monocluster-based structure. The asymmetric unit contains one Nd^{3+} ion, two phacac ligands, two phen ligands, and a half SO_4^{2-} anion (Fig. 2a). The central Nd^{3+} ion is coordinated by four oxygen atoms from two phacac ligands and four nitrogen atoms from the two phen ligands, giving a square antiprism coordination geometry. The Nd^{III}–O bond distances are in the range of 2.339(2) to 2.378(3) and the Nd^{III}–N bond lengths are in the range of 2.609(2) to 2.699 (2) Å, which all locate in the normal range of the Nd–O and Nd–N bond distances in other Nd^{III}-based coordination complexes.[19–21] The two phacac ligands reveal two different geometries: one with the two benzene rings twisting with each other at a dihedral angle of 38.6°, the other one with the two benzene rings twisting with each other with a dihedral angle of 21.4° (Fig. 2b). It could be observed that the C–C bond distances for the carbonylic C atoms are in the range of 1.372(11) to 1.387(11) Å, which indicates that both of the phacac ligands in the structure of **2** are deprotonated. As for the phen ligands, they chelate with the Nd^{3+} ion in the same direction and reveal a π–π interaction with a distance of 3.923 Å (Fig. 2c). The structure of **2** is further extended into a 1D chain-like structure via the π–π interactions, which are contributed by the benzene rings on the phen ligands and the phacac ligands (Fig. 2d).

*PXRD, TGA, and Reduction in Size of Complexes **1** and **2***

To characterise the phase purities of the as-prepared two compounds, the corresponding PXRD patterns were collected at room temperature. As shown in Fig. 3a, the experimental patterns of compounds **1** and **2** show good agreement with the simulated ones calculated from the single crystal X-ray data, revealing that the as-prepared two compounds are in their pure phase states. To characterise the compounds more fully in terms of thermal stability, we have examined the TGA for compounds **1** and **2** under N_2 atmosphere in the temperature range of 30–800°C (Fig. 3b). The TGA curve for **1** shows that there is a weight loss of 5.3 % from room temperature to 152°C, which

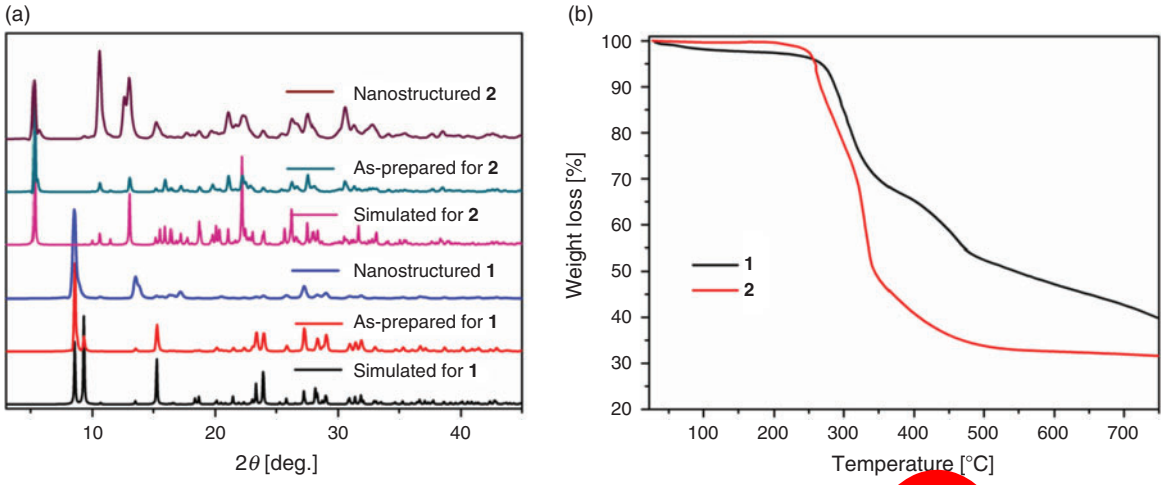

Fig. 3. (a) The PXRD patterns for compounds **1** and **2**. (b) The TGA curves for co[illegible]unds **1** [illegible] **2**.

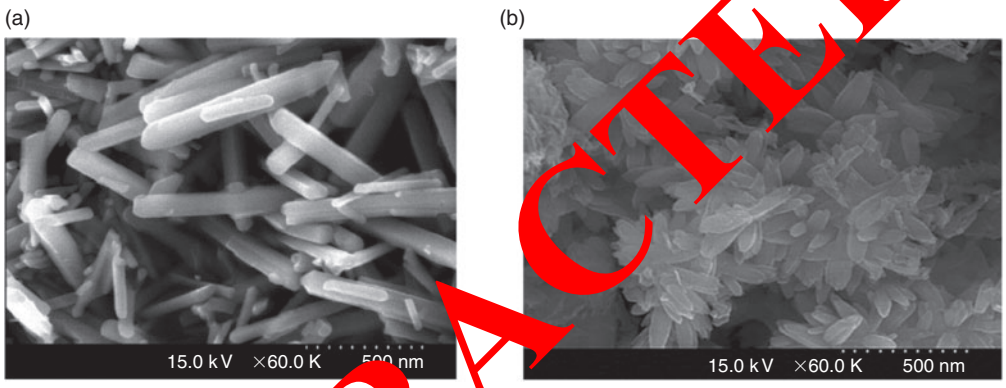

Fig. 4. [illegible] SEM [illegible] for the nanocrystalline **1** (a) and **2** (b).

could be due to the removal of two tolue[illegible] molecules in the crystal lattice. An abrupt weight loss could b[illegible]served after a long plateau from 160 to 2[illegible]7°C, indicating that the whole structure has decomposed. Th[illegible]G[illegible] curve for **2** shows there is no obvious weight loss until a te[illegible]rature of 244°C, indicating that there is no solvent [illegible] the cry[illegible] lattice of **2** and this is consistent with the [illegible]lts [illegible] the SCXRD study and elemental analysis.

Considering the follo[illegible]g cytotoxicity tests, it is necessary to reduce the size of compounds **1** and **2** to the nanometre scale, which could facilitate the release of drugs to the whole body and allow absorption by specific tissues by intravenous administration. As shown in Fig. 4, nanocrystalline **1** and **2** were prepared by a grinding method at room temperature and were characterised by scanning electron microscopy (SEM). The PXRD reflections of the obtained nanocrystalline **1** and **2** correspond well with the simulated patterns, readily indexing the high crystallinity of the obtained nanomaterials. The nanocrystalline **1** and **2** adopt almost rod-like morphologies in order to minimise the interfacial free energy between the particle and the solvent molecules, and the average thickness of the two nanostructures is 60 and 50 nm, respectively.

MTT Assay

MTT assays were performed to investigate the toxicity of nanocrystalline **1** and **2** towards the cancer cell line SW60.

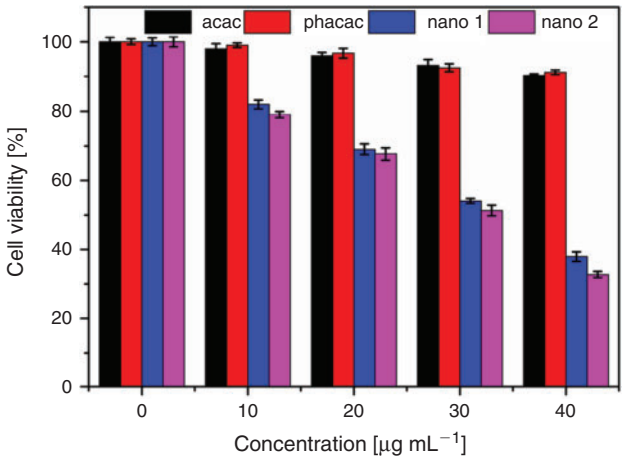

Fig. 5. The IC_{50} values for different compounds.

Compounds were dissolved in DMSO and blank samples containing the same volume of DMSO were taken as controls to identify the activity of solvent in this cytotoxicity experiment. Different concentrations of nanocrystalline **1** or **2** were cultured with SW60 cells. As shown in Fig. 5, the cell viability of the group cultured with acac and phacac ligands remained high even at a high concentration, showing that the organic ligands are

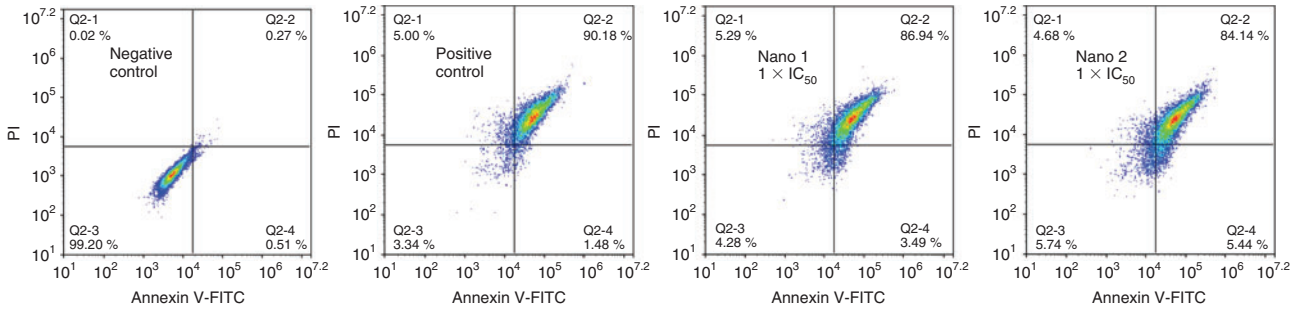

Fig. 6. Both nanocrystalline **1** and **2** ($1 \times IC_{50}$) can induce SW60 cell death via apoptosis.

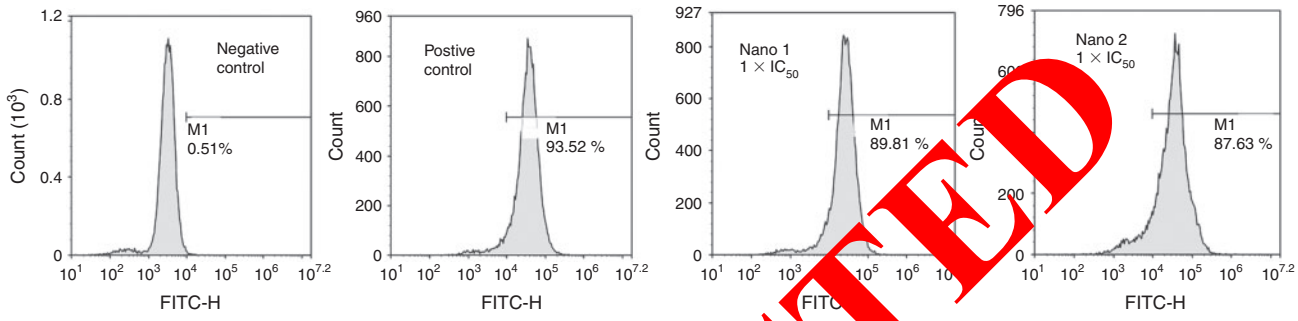

Fig. 7. The ROS levels in SW60 cells after incubation with nanocrystalline **1** and **2** ($1 \times IC_{50}$) were measured with flow cytometry.

non-toxic in nature. However, as the concentration of nanocrystalline **1** increases, the cell viability decreases, and the IC_{50} (half-maximal inhibitory concentration) is approximately 38 μg mL^{-1} for nanocrystalline **1**. For the group incubated with nanocrystalline **2**, a comparable IC_{50} was observed (36 μg mL^{-1}), demonstrating that both nanometre-sized coordination complexes show promising anticancer activities.

Nanocrystalline **1** and **2** both showed a significant inhibitory effect on cancer cells. Flow cytometry was used to quantify the percentages of apoptotic SW60 cells labelled with Annexin V-FITC/PI dyes (Fig. 6). After treatment with nanocrystalline **1** or **2**, there are increased levels of apoptotic cells compared with the control group ($P < 0.05$ or $P < 0.01$) at a percentage of 20.8 ± 2.4 and 40.6 ± 2.1% respectively. Thus the Annexin V/PI double staining assay confirmed that the complexes could induce cell death via apoptosis in SW60 cells. We then explored if the apoptosis of the cells was due to increased ROS production in the SW60 cells. The treatment groups showed a higher level of ROS than the control one (Fig. 7). All the results indicated that both nanocrystalline **1** and **2** have antitumour activities. This effect is a result of the significant increase of intracellular ROS and subsequent cell apoptosis.

Crystallographic Data

CCDC Nos. 1878788 and 1878789 contain the supplementary crystallographic data for this paper. These data can be obtained free of charge at www.ccdc.cam.ac.uk/conts/retrieving.html (or from the Cambridge Crystallographic Data Centre, 12, Union Road, Cambridge CB2 1EZ, UK; fax: (internat.) +44 1223/336 033; email: deposit@ccdc.cam.ac.uk).

Conclusion

In summary, two novel lanthanide–organic complexes with discrete structures have been successfully prepared and characterized. In complex **1**, four lanthanide atoms, four μ_3-O atoms, and eight acac ligands make up the peripheral part of the cage-like $Ho_4(\mu_3\text{-}OH)_4^{8+}$ cluster core with the acac ligands showing two different types of structural conformations. In complex **2**, the central Nd^{3+} ion is eight-coordinated by four O atoms from two different phacac ligands and four N atoms from two different phen ligands, giving a square antiprism coordination geometry. Furthermore, the morphology of the two complexes could be conveniently decreased to the nanometre scale by grinding. Moreover, nanocrystalline **1** and **2** have been found to show promising toxicity towards the colon cancer cell line SW60, indicating their potential application as anticancer reagents in the future.

Conflicts of Interest

The authors declare no conflicts of interest.

Acknowledgements

This work was supported by grants from the Foundation of Heilongjiang Provincial Natural Science of China (No. H201367), the Postdoctoral Foundation of Heilongjiang Province of China (No. LBH-Z15152), and the Postdoctoral Research Start-up Fund of Heilongjiang Province of China (No. LBH-Q17160).

References

[1] L. A. Torre, F. Bray, R. L. Siegel, J. Ferlay, J. Lortet-Tieulent, A. Jemal, *CA Cancer J. Clin.* **2015**, *65*, 87. doi:10.3322/CAAC.21262
[2] S. H. van Rijt, P. J. Sadler, *Drug Discov. Today* **2009**, *14*, 1089. doi:10.1016/J.DRUDIS.2009.09.003
[3] P. C. A. Bruijnincx, P. J. Sadler, *Curr. Opin. Chem. Biol.* **2008**, *12*, 197. doi:10.1016/J.CBPA.2007.11.013
[4] K. G. Daniel, P. Gupta, R. H. Harbach, W. C. Guida, Q. P. Dou, *Biochem. Pharmacol.* **2004**, *67*, 1139. doi:10.1016/J.BCP.2003.10.031
[5] C. X. Zhang, S. J. Lippard, *Curr. Opin. Chem. Biol.* **2003**, *7*, 481. doi:10.1016/S1367-5931(03)00081-4

[6] D. M. Chen, N. N. Zhang, C. S. Liu, M. Du, *J. Mater. Chem. C Mater. Opt. Electron. Devices* **2017**, *5*, 2311. doi:10.1039/C6TC05349A
[7] X. L. Li, C. L. Chen, Y. L. Gao, C. M. Liu, X. L. Feng, Y. H. Gui, S. M. Fang, *Chem. – Eur. J.* **2012**, *18*, 14632. doi:10.1002/CHEM.201201190
[8] Y. Yang, F. Jiang, L. Chen, J. Pang, M. Wu, X. Wan, J. Pan, J. Qian, M. Hong, *J. Mater. Chem. A Mater. Energy Sustain.* **2015**, *3*, 13526. doi:10.1039/C5TA00720H
[9] H. Ke, L. Zhao, Y. Guo, J. Tang, *Inorg. Chem.* **2012**, *51*, 2699. doi:10.1021/IC202699K
[10] M. Y. Guo, X. Zhang, L. Zhao, Y. K. Li, D. Y. Chen, G. W. Yang, Q. Y. Li, *J. Solid State Chem.* **2018**, *259*, 104. doi:10.1016/J.JSSC.2018.01.006
[11] K. M. Park, H. Kim, J. Murray, J. Koo, K. Kim, *Supramol. Chem.* **2017**, *29*, 441. doi:10.1080/10610278.2016.1266359
[12] F. Duan, X. Feng, X. Yang, W. Sun, Y. Jin, H. Liu, K. Ge, Z. Li, J. Zhang, *Biomaterials* **2017**, *122*, 23. doi:10.1016/J.BIOMATERIALS.2017.01.017
[13] C. Shiju, D. Arish, S. Kumaresan, *Arab. J. Chem.* **2017**, *10*, S2584. doi:10.1016/J.ARABJC.2013.09.036
[14] S. Mukherjee, S. Ganguly, K. Manna, S. Mondal, S. Mahapatra, D. Das, *Inorg. Chem.* **2018**, *57*, 4050. doi:10.1021/ACS.INORGCHEM.8B00237
[15] G. M. Sheldrick, *SHELX-97: Program for the Solution and Refinement of Crystal Structures* **1997** (University of Göttingen: Göttingen).
[16] H. Chen, S. Adams, *IUCrJ* **2017**, *4*, 614. doi:10.1107/S2052252517010211
[17] S. Quici, M. Cavazzini, G. Marzanni, G. Accorsi, N. Armaroli, B. Ventura, F. Barigelletti, *Inorg. Chem.* **2005**, *44*, 529. doi:10.1021/IC0486466
[18] X.-L. Li, F.-C. Li, X.-L. Zhang, Y.-F. Liu, A.-L. Wang, J.-F. Tian, H.-P. Xiao, *Synth. Met.* **2015**, *209*, 220. doi:10.1016/J.SYNTHMET.2015.07.035
[19] Y. Feng, H. Fan, Z. Zhong, H. Wang, D. Qiu, *Inorg. Chem.* **2016**, *55*, 11987. doi:10.1021/ACS.INORGCHEM.6B02117
[20] Y. Feng, M. Li, H. Fan, Q. Huang, D. Qiu, H. Shi, *Dalton Trans.* **2015**, *44*, 894. doi:10.1039/C4DT02840F
[21] C. W. Duan, L. X. Hu, J. L. [illegible] *Mater. Chem. A Mater. Energy Sustain.* **2018**, *6*, 6309. doi:10.103[illegible]TA00533H